IOP Conference Series: Earth and Environmental Science

Unsteady pressure measurements of decelerated swirling flow in a discharge cone at lower runner speeds

To cite this article: A I Bosioc *et al* 2014 *IOP Conf. Ser.: Earth Environ. Sci.* **22** 032008

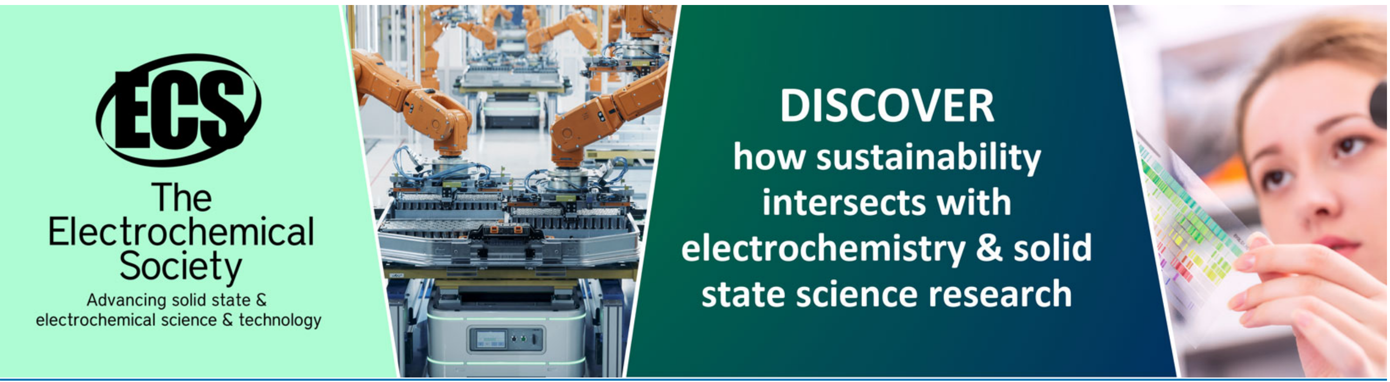

Unsteady pressure measurements of decelerated swirling flow in a discharge cone at lower runner speeds

A I Bosioc[1], S Muntean[2], C Tanasa[1] , R Susan-Resiga[1,2] and L Vékás[2]
[1] Department of Hydraulic Machinery, University Politehnica Timisoara, Bv. Mihai Viteazu, No. 1, Ro-300222, Timisoara, Romania
[2] Center for Advanced Research in Engineering Sciences, Romanian Academy – Timisoara Branch, Bv. Mihai Viteazu, No. 24, Ro-300223, Timisoara, Romania

E-mail: alin.bosioc@upt.ro

Abstract. The decelerated swirling flow in the draft tube cone of hydraulic turbines (especially turbines with fixed blades) is responsible for self-induced instabilities which generates pressure pulsations that hinder the turbine operation. An experimental test rig was developed in order to investigate the flow instabilities. A new method was implemented to slow down the runner using a magneto rheological brake in order to be extended the flow regimes investigated. As a result, the experimental investigations are performed for 7 operating regimes in order to quantify the flow behaviour from part load operation to overload operation. The unsteady pressure measurements are carried out on 4 levels in the cone. The unsteady pressure measurements on the cone wall consist in quantifying of three aspects: i) the pressure recovery coefficient obtained based on mean pressure provides the energetic assessment on the draft tube cone; ii) the unsteady quantities (dominant amplitude and frequency) are determined revealing the dynamic behaviour; iii) the plunging and rotating components of the pressure pulsation. As a result, this new method helps us to investigate in detail the flow instability for different operating regimes and allows investigating various flow control solutions.

1. Introduction

Currently there is a growing demand for renewable energy in the industrialized countries. However, these energy sources (e.g. solar, wind) introduce a fluctuating behaviour in the grid. Therefore, the hydraulic turbines have to operate far away from the best efficiency point (BEP) covering a wide area. An important component of the hydraulic turbines with low and medium head is the draft tube cone due to the most important energy is recovered along to this part [1]. The hydraulic losses increase sharply with a significant decrease in efficiency when the turbines operate far away from the best efficiency point. Also, the self induced instabilities are generated in the draft tube cone (e.g. vortex rope) leading to strong pressure pulsations.

Different control methods have been introduced and tested in order to mitigate the vortex rope effects. Kurokawa et al. [2] proposed J-Groove method which consists in mounting radial groves on the draft tube cone. Thike [3] and Falvey [4] have tested different extensions of runner cone to suppress the stagnant region and associated vortex rope. Recently, a new control method was proposed [5] and successfully tested experimentally which involves using an axial water jet to the runner cone [6]. The results clearly showed that using the optimum amount of jet water, the stagnant region and the vortex rope are completely eliminated from the draft tube cone. Foroutan and Yavuzkurt [7] have reached at a similar conclusion, when tested numerically water injection method on a Francis turbine.

The vortex rope effects are present both at partial discharge and at full load discharge. The experimental test rig developed in laboratory was design to investigate one operating regime. A new solution was tested by lowering the runner speed in order to extend the investigation at several swirling flow configurations. This solution covers a wide range of discharge values from 0.7 up to 1.54 from best efficiency point discharge at constant guide vane opening.

The unsteady pressure field associated to several swirling flow configurations into the discharge cone is investigated. The design and implementation of the magneto-rheological break (MRB) system on the test rig is presented in section 2. The experimental setup for unsteady pressure measurements is described in section 3. The unsteady pressure data and their analysis are included in section 4, while the conclusions are drawn in last section.

2. Experimental test rig and magneto-rheological brake (MRB) system.

An experimental test rig was developed at Politehnica University of Timisoara in order to investigate different methods for controlling the vortex rope. However, it was designed and installed a swirl generator instead of using a Francis turbine model.

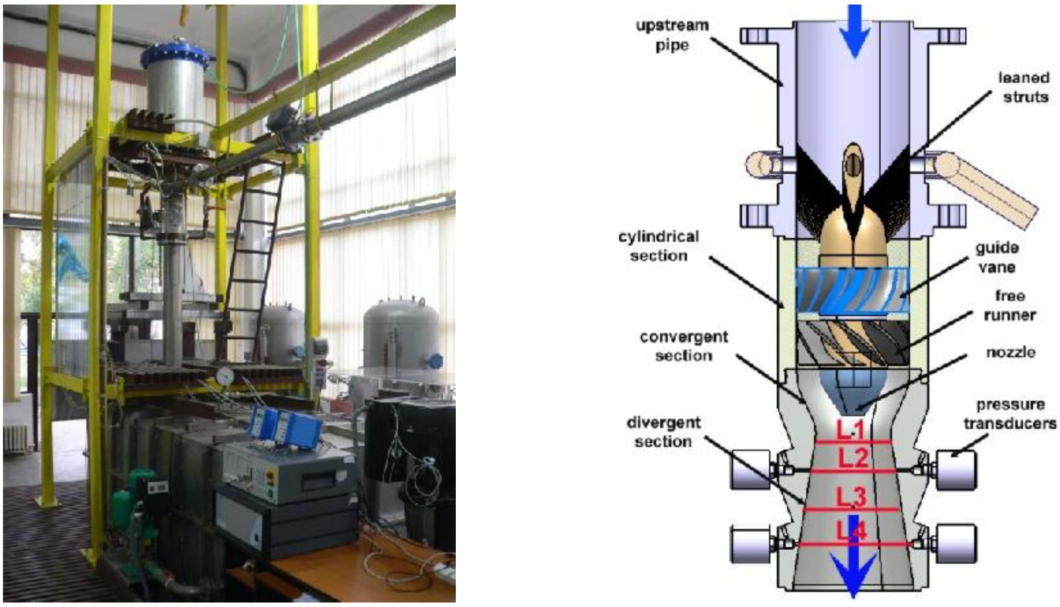

Figure 1. Experimental test rig developed for decelerated swirling flows analysis (left) and sketch of the swirl apparatus with main components and the name of pressure levels (right)

Our swirl apparatus includes two main parts: the swirl generator and the test section, like in Figure 1, [6]. The swirl generator contains an ogive with four struts, a guide vane with 13 blades and a runner with 10 blades which spins freely delivering at the discharge cone inlet a flow configuration similar with a Francis runner at partial discharge (approximately 70% from the BEP), [8]. The swirl generator ends with a nozzle used to investigate different control methods in order to mitigate the vortex rope, [9, 10]. On the other side, the test section contains a cylindrical part where is installed the swirl generator followed by a convergent-divergent part. The divergent part of the test section was designed with the included cone angle of 17°=2×8.6°, similar to the real discharge cone of a Francis turbine draft tube.

A magneto-rheological brake (MRB) system was designed and installed in order to control the runner speed. As a result, the runner speed is decreased up to 70% using the MRB system providing several swirling flow configurations at the discharge cone inlet covering a wide range (from part load to full load conditions).

The dimensionless flux of moment of momentum distribution versus dimensionless discharge was computed for several runner speed values based on experimental data, see Figure 2 (rigth). The same distribution is obtained for FLINDT Francis turbine proving the same behaviour for the swirl generator [11], Figure 2 (left). The dimensionless discharge q is determined using following formula:

$$q = \frac{Q}{\mu \cdot \text{®} \cdot R_{ref}^{3}} \ , Q = \int_A \vec{V} \cdot \vec{n} \, dA \quad (1)$$

where, μ is radial speed of the runner, R_{ref} is runner radius, $\vec{V}$ represent the velocity vector and $\vec{n}$ normal unit vector. The dimensionless flux of moment of momentum was computed using the Eq. (2):

$$m_2 = \frac{M}{(\mu \cdot R_{ref})^3 \cdot \text{®} \cdot R_{ref}^2} \ , M = \int_A (U \cdot V_u) \vec{V} \cdot \vec{n} \, dA \quad (2)$$

where M is the dimensional flux of moment of momentum, being determined just downstream of the runner based on LDV data, A is the cross section, V_u is the tangential velocity and $U = \mu R$ is the transport velocity. As is observed in Figure 2 (rigth), at a runner speed value around 600 rpm the dimensionless flux of moment of momentum has a vanishing value which from operating point of view, the runner works close to BEP. Four regimes corresponding to runner speed values of 925 rpm, 840 rpm, 800 rpm and 700 rpm are associated to the partial operating conditions with a positive m_2. When the runner is slow down more than 600 rpm, the m_2 starts to have an inverse value, which it means that the runner starts to act as a hydraulic turbine operated at full load operation.

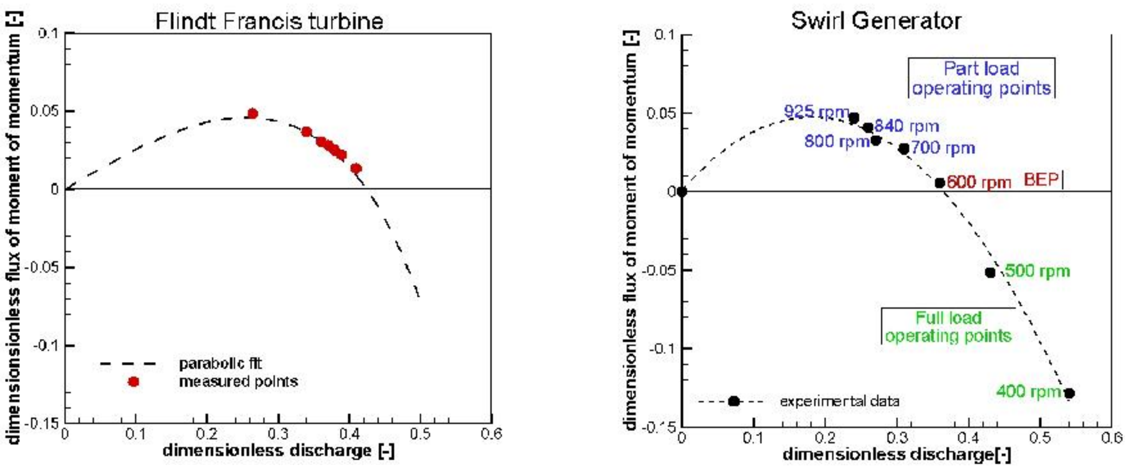

Figure 2. Dimensionless flux of moment of momentum calculated for FLINDT Francis turbine (left) and dimensionless flux of moment of momentum calculated for our swirl generator (right)

The intermediate values for runner speed and corresponding dimensionless discharge is presented in the next table.

Table 1. Runner speeds and corresponding operating regimes.

Runner speed n [rpm]	925	840	800	700	600	500	400
Operating regimes depending by m_2	positive $m_2>0$	positive $m_2>0$	positive $m_2>0$	positive $m_2>0$	vanishing $m_2\sim0$	negative $m_2<0$	negative $m_2<0$
Dimensionless discharge q [-]	0.23	0.248	0.27	0.309	0.36	0.342	0.54
Discharge coefficient with respect to BEP value [-]	0.7 (part load)	0.74 (part load)	0.75 (part load)	0.86 (part load)	1 (BEP)	1.19 (full load)	1.5 (full load)

As previously stated, the speed of the runner is reduced using a MRB system. This solution was chosen because have some advantages as: small and robust, no mechanical parts, fast response time in order to control and low power consuming. In our case all system was especially designed, because was adapted to our geometric constraints and we benefit by the experience of Magneto-Rheological Laboratory from our department. As a working principle, a magneto-rheological (MR) fluid is mounted between a rotating and a fixed piece. When a magnetic field (usually generated by a coil) is passing, the MR fluid is changing viscosity. Depending by the intensity of the magnetic field the viscosity is changing which makes that the rotating part to reduce the speed. A sketch with the MRB system and assembled components are presented in Figure 3.

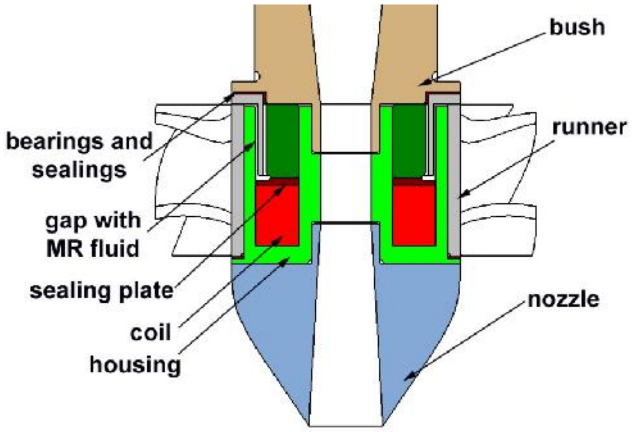

Figure 3. Sketch of the MRB system (left) and picture with mounted pieces (right)

The runner was manufactured so that to be mounted the MRB system. The MRB system consists in iron housing, a coil, seals and bearings and the MR fluid. The housing is made of iron and was design in order to close the magnetic field in the area where MR fluid is mounted. The coil is made by cupper wires and a custom program was used to choose the number of wires and the wire thickness. A series of seals were used to keep the MR fluid separated by water (all system is surrounded by water), also these seals were used as bearings. The most important component by all system is the MR fluid. We have chosen a MR fluid produced by LORD Corporation (MRF 336 AG). For the MR brake controlling the speed of the runner a quantity of 20 ml of MR fluid was necessary. The gap between rotating and fixed part is 1 mm and time response of the entire system is lower than 0.1 sec. Because the MRB system is working in water, no cooling system is necessary. A DC power supply with a maximum electrical voltage of 30V and a maximum electrical current of 5 A was used in order to control the magnetic field of the MR brake.

3. Pressure measurements setup

The purpose of this research is to assess the swirling flow from a draft tube cone at different operating regimes. The measured unsteady pressure is used to analyse the dynamic and energetic performances. With mean pressure is calculated the pressure recovery coefficient, the flow from the draft tube cone being analysed from energetically point of view. The unsteady pressure is used to calculate the amplitude, frequency and type of the conical diffuser unsteadiness, the flow from the draft tube cone being analysed from dynamically point of view. After MRB system was installed and tested on the test rig, the pressure test section was mounted in order to perform experimental investigations. The top level located in the test section throat is considered the reference for pressure measurements and was noted L1, according with Figure 1 (right). The rest of levels L2, L3 and L4 correspond to 50, 100 and 150 mm downstream in the draft tube cone, relative with L1. Eight capacitive pressure sensors were

installed on the divergent part. Each level contains two opposite pressure sensors, in order to establish that pressure sensors indicate same static pressure and determine type of unsteadiness from the draft tube cone. They have an accuracy of ±0.13% within a range of ±1 bar relative pressure. A main operating discharge of 30 l/s was used in experiments for all operating regimes. The speed of the runner was reduced from 925 up to 400 rpm being respected the regimes presented in
Table 1. In order to check repeatability 10 experiments were performed for each regime. Each set corresponds to an acquisition time of 32s at a sampling rate of 256 samples/s.

4. Results and analysis

From experimental investigation, a first analysis is to evaluate the energetic flow behaviour from the draft tube cone from part load regime (corresponding to design speed) up to full load regime (corresponding to lower runner speeds). The pressure recovery coefficient takes into account mean pressure and is calculated with following equation:

$$c_p = \frac{\overline{p} - \overline{p}_{L1}}{\rho \cdot \frac{v_t^2}{2}} \tag{3}$$

where c_p is the pressure recovery coefficient, $\overline{p}_{L1}$ is mean the pressure recorded at L1 level, $\overline{p}$ is the measured pressure downstream L1 level, ρ is the water density and v_t the bulk velocity in the throat section.

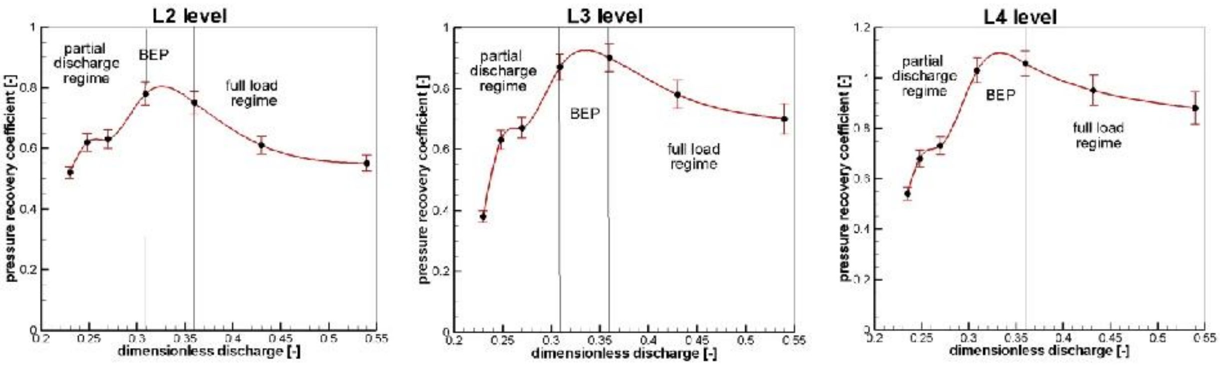

Figure 4. Pressure recovery coefficient on L2, L3 and L4 levels depending by dimensionless discharge

Figure 4 presents the variation of pressure recovery coefficient in three investigated levels: L2, L3 and L4. For all levels at partial discharge regimes the pressure recovery has a maximum of 0.7 in L4 level. When is reached at BEP the pressure recovery has maximum values in all levels, which confirm the role of the cone (to convert kinetic into pressure energy). When is reaching at full load regime the pressure recovery coefficient starts to decrease once that departing from BEP, nevertheless due not reach at minimum values from partial discharge regimes. Figure 5 present an evolution of pressure recovery coefficient in the length of the cone for three distinct cases. As is observed at partial discharge regime the role of the cone is functional only in the first third of the cone. At full load the cone recovers energy in all length of the cone with 0.75 less than at BEP. At partial discharge regime (q=0.23, for example) the pressure recovery coefficient is with 0.5 less approximately than BEP case.

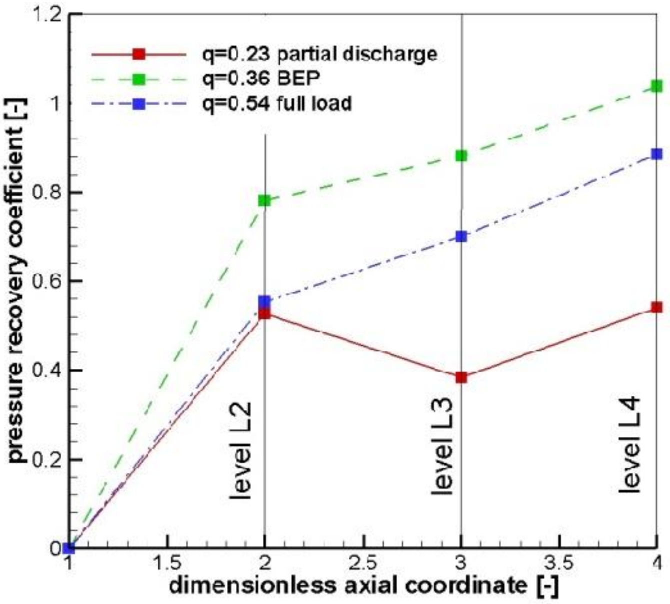

Figure 5. Evolution of pressure recovery coefficient at three distinct regimes in dimensionless length of the draft tube cone.

A second pressure analysis is to investigate the flow from dynamical point of view. From the pressure signal was extracted the Fourier spectra. A new approach is employed to emphasize this signal. A second signal is reconstructed based on the acquired one, using the Parceval's theorem. The reconstructed signal has the same frequency as the first harmonic of the acquired signal and root mean square equivalent amplitude. A detailed analysis with this method is presented in [6].
For a discrete signal the amplitude and pressure fluctuations dimensionless form are defined as:

$$p_a = \frac{p_A}{\rho \cdot \frac{v_t^2}{2}} \tag{4}$$

where p_A represent the dimensional pressure amplitude or pressure fluctuation and the rest of terms are previously stated.

The second dimensionless parameter to be used is the Strouhal number, defined as:

$$Sh = f \cdot \frac{D_t}{v_t} \tag{5}$$

with f being the frequency of the flow from draft rube cone and D_t throat diameter of test section.

Dimensionless equivalent amplitude (Figure 6 left) shows that at partial regimes different values are recorded depending by measured level. On L2 level and L3 level are situated the maximum amplitudes for partial regimes, which it means that in the middle of the cone the vortex rope has the maximum eccentricity. At BEP the equivalent amplitude is approximately identical for first three levels. As a result the flow instabilities at this operating regime have no influence in the cone. When is operated at full load regimes the equivalent amplitudes start to increase, having distinct values for each level. For L1 level the amplitude is approximately 4.5 times larger than at BEP, for L2 level 3 times larger, for L3 2 times larger, while at L4 level remain identical. Also for q = 0.54 (full load regime) the amplitudes generates vibrations sensed in all experimental test rig. In case of registered Strouhal noumber which is constant in all investigated levels of the cone, first at part load regime is decreasing reaching at a value of 0.7 smaller than at minimum q. As a comment is that at minimum q (925 rpm) the Strouhal number of the runner is similar with Strouhal number of the flow from the cone. When speed is reduced and q starts to increase the Strouhal number of the runner is different by Strouhal number of the flow from the cone. At full load regime the Strouhal number of the flow from the cone is increasing once that q increasing.

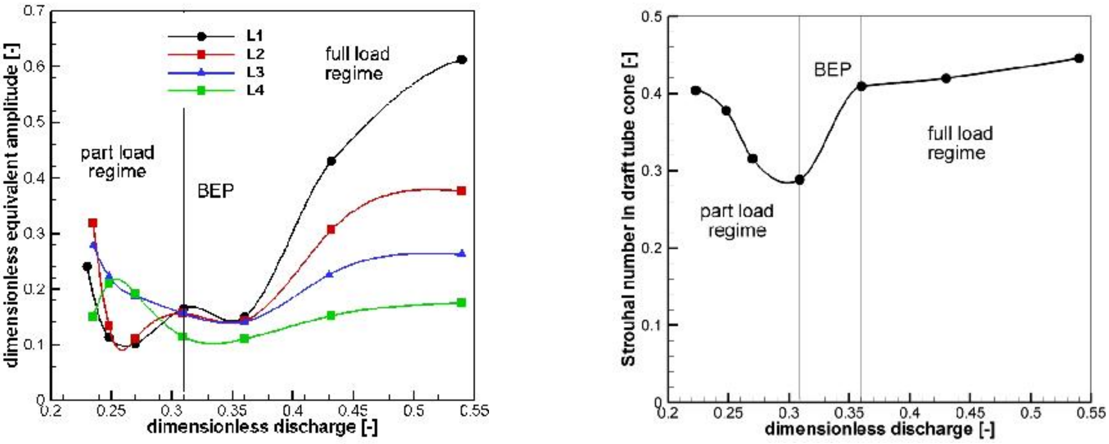

Figure 6. Dimensionless equivalent amplitude and Strouhal number for all levels depending by dimensionless discharge.

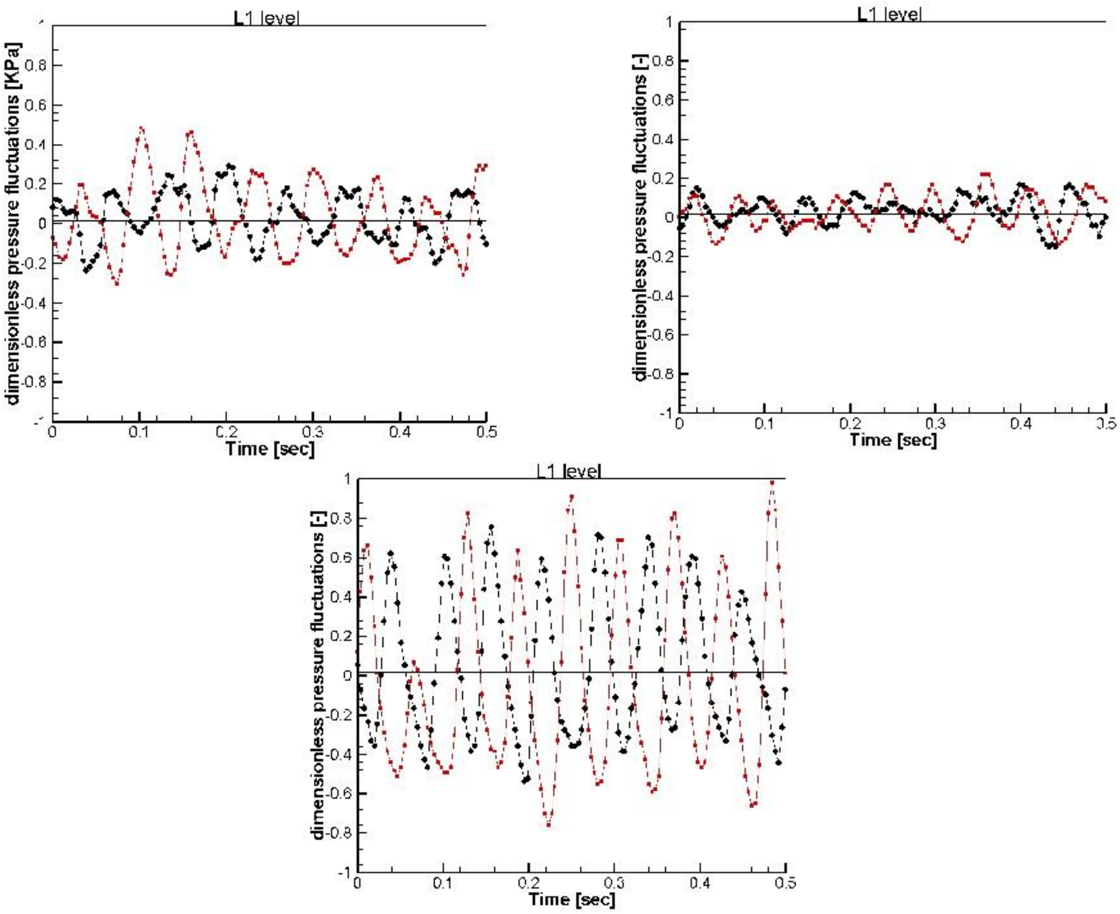

Figure 7. Registered dimensionless pressure fluctuations for L1 levels at three distinct flow regimes: part load regime q=0.23 (top left), BEP q=0.36 (top right) and full load q=0.54 (bottom).

A last analysis consists in evaluation of signal decomposition, keeping into account that on each level two pressure signals are registered on opposite sides. According with Jacob and Prenat [12], there are two types of draft tube cone pulsations. The plunging type is acting as a water hammer in the length of the cone, while the rotating type is acting in the cross sections of the cone. The rotating type is produced by flow instabilities as vortex rope due to its shape. First are represented both dimensionless pressure signals on same level. Figure 7 present an example of haw appears the registered signals for L1 level at three representative dimensionless discharges.

The decomposition procedure to obtain rotating and plunging pulsation types is described in Bosioc et al. [6]. Also for pressure pulsations decomposition from the experimental data was using the procedure based on the Parceval's theorem.

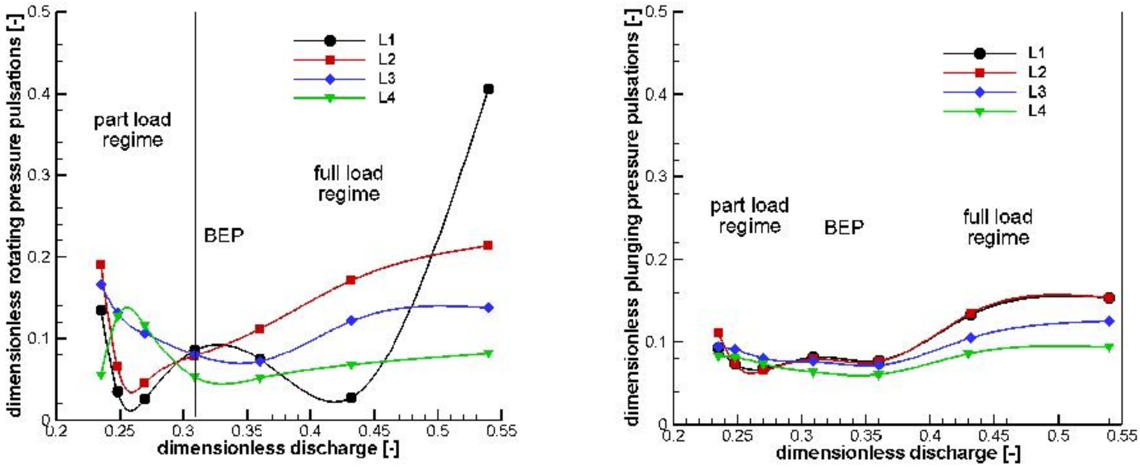

Figure 8. Dimensionless pressure signal decomposition into rotating (left) and plunging (right) type in all levels at different operating regimes.

The rotational component of pressure pulsation associated with the vortex rope is significant for part load regime and full load regime especially in first three levels. If at part load regime the pressure fluctuation given by the vortex rope is higher in the middle of the cone (L2 and L3) levels, when is reaching at full load regime the largest pulsation is registered at the cone throat. This significant decrease and level modification is given by the stagnant region which at full load is increasing in throat cone region, [13]. Once that stagnant region increase close to the throat also the plunging type pulsation is increasing.

5. Conclusions

The paper presents experimental measurements of decelerated swirling flow in a conical diffuser at different operating regimes. The speed of the runner of the swirl generator was controlled by a MR brake system. Accordingly with dimensionless discharge and dimensionless flux of moment of momentum, when the runner speed is reduced, it acts as a real runner operating from part load (design operation) up to overload regimes at constant guide vane opening.

The pressure measurements were made in four levels in the cone, each level having two opposites' pressure transducers. The results are analyzed from two points of view: energetically and dynamically. From energetic point of view is calculated the mean pressure resulting pressure recovery coefficient. The amplitude, frequency and signal decomposition help to characterize the flow from dynamic point of view. Pressure recovery coefficient shoved clearly that when the runner is operated at partial regime the static pressure is recovered only in the first part of the cone, being observed only 50% pressure recovery than in BEP case. At full load regime the pressure recovery is at 75% in comparison with BEP. In the case of dynamical analysis, the equivalent amplitude has maximum values in the middle of the cone when is working at partial discharge. This results from the shape of the vortex rope, with maximum eccentricity in the middle of the cone. At BEP the amplitudes registered same values in all length of the cone, while at full load regime the maximum amplitude is registered at throat cone. This analysis cumulated with pressure signal discrimination showed that at full load regime the vortex rope has maximum amplitude at throat level, which conducts to increase of stagnant region from this part of the cone.

Therefore, the paper presents a new approach by using a swirl generator in order to obtain a flow configuration in the draft tube cone as a real runner operated at variable discharge. This approach helps us to investigate in detail the flow instability for different operating regimes and allows investigating various flow control solutions.

Acknowledgments

This work was supported by a grant series of the Romanian National Authority for Scientific Research, CNCS – UEFISCDI, projects numbers PN-II-RU-PD-2011-3-0165, PNII-ID-PCE-2012-4-0634 and by the project MagNanoMicroSeal Program PN-II – PCCA – type2 –Ctr. Nr. 157/2012. Dr. Constantin Tanasa was partially supported by the strategic grant POSDRU/159/1.5/S/137070 (2014) of the Ministry of National Education, Romania, co-financed by the European Social Fund – Investing in People, within the Sectoral Operational Programme Human Resources Development 2007-2013."

References

[1] Vu T C and Retieb S 2002 Accuracy assessment of current CFD tools to predict hydraulic turbine efficiency hill chart, in Proc. of the 21st IAHR Symposium on Hydraulic Machinery and Systems, (Lausanne, Switzerland), 193-198.

[2] Kurokawa J, Kajigaya A, Matusi J and Imamura H 2000 Supression of the swirl in a conical diffuser by use of J-Groove in Proc. of the 20th IAHR Symposium on Hydraulic Machinery and Systems, (Charlotte, North Carolina, USA)

[3] Thike R H 1981 Practical solutions for draft tube instability Water Power and Dam Construction, 33(2), 31-37

[4] Falvey H T and Cassidy J J 1970 Frequency and amplitude of pressure surges generated by swirling flows, in Proc. of 5th Symposium of International Association for Hydraulic Machinery, Equipments and Cavitation, (Stockholm Sweden), E1

[5] Susan-Resiga R F, Vu T C, Muntean S, Ciocan G D and Nennemann B 2006 Jet control of the draft tube vortex rope in Francis turbines at partial discharge, in Proc. of the 23rd IAHR Symposium on Hydraulic Machinery and Systems, (Yokohama, Japan), F192.

[6] Bosioc A I, Susan-Resiga R F, Muntean S and Tanasa C 2012 Unsteady Pressure Analysis of a Swirling Flow with Vortex Rope and Axial Water Injection in a Discharge Cone, ASME J. Fluids Eng., 134, 081104.

[7] Foroutan H and Yavuzkurt S 2014 Flow in the simplified draft tube of a Francis turbine operating at partial load. Part 2. Control of the vortex rope, J. Applied Mechanics, 81(6), 061011.

[8] Ciocan G, Iliescu M, Vu T C, Nennemann B and Avellan F 2007 Experimental study and numerical simulation of the FLINDT draft tube rotating vortex, ASME J. Fluids Eng., 129, 146-158.

[9] Bosioc A I, Tanasa C, Muntean S and Susan-Resiga R F 2010 Unsteady Pressure Measurements and Numerical Investigation of the Jet Control Method in a Conical Diffuser with Swirling Flow, in Proc of the 25th IAHR Symposium on Hydraulic Machinery and Systems, (Timisoara, Romania), online at: IOP Conf. Series: Earth and Environmental Science, 12, 012017.

[10] Tanasa C, Susan-Resiga R F, Muntean S and Bosioc A I 2013 Flow-Feedback Method for Mitigating the Vortex Rope in Decelerated Swirling Flow, ASME J. Fluids Eng., 135, 061304

[11] Susan Resiga R, Muntean S, Avellan F and Anton I Mathematical modelling of swirling flow in

hydraulic turbines for the full operating range, Applied Mathematical Modelling, 35, 4759-4773.

[12] Jacob T 1993 Evaluation sur modele reduit et prediction de la stabilite de functionnement des turbines Francis, PhD. Thesis, (Laussane, Switzerland).

[13] Bosioc A I, Muntean S, Susan-Resiga R F, Vekas L and Bernad S 2013 Numerical Simulation of the Swirl Generator Discharge Cone at Lower Runner Speeds, in Proc. of the 11th International Conference of Numerical Analysis and Applied Mathematics, 8th Symposium on Numerical Analysis of Fluid Flow and Heat Transfer, (Rhodos, Greece), online at AIP Conference Proceedings, 1558, 204.